Scientia Iranica, Vol. 6, No. 1, pp 18–24

SCIENTIA
IRANICA

Design and Performance of Permanent Magnet Motors for High Efficiency Industrial Drives

M. Mirsalim* and C.T. Mi[1]

Permanent Magnet (PM) motors offer potential energy savings through higher efficiency compared with the industry standard induction motors. Advances in rare-earth PM materials and power electronics serve to improve the PM motors' cost competitiveness, making them practical for general purpose industrial applications. This paper describes the electromagnetic design and construction through exploring ways of reducing the cost and material consumption of high efficiency PM motors. The choice of magnetic material, number of slots and number of poles are among the parameters identified as critical in achieving this goal. In order to consider saturation, iron losses and space harmonics, Finite Element (FE) analysis is used. Design guidelines and the presented results are supported by experimental testing of a prototype 2.3 HP machine.

INTRODUCTION

There was very little interest in PM machines for drive systems two decades ago. It was only when rare-earth magnets with high energy products exceeding 0.35 MJ/m^3 became available that industry recognized that PM machines were not simply low power devices of minor commercial importance [1]. PM motors are presently widely used in variable speed drives, position control systems and robotics due to their high dynamic performance and superior controllability [2]. However, there has not been much movement to use the motors in general purpose industrial applications due to their higher initial cost compared to induction motors. Recent developments and cost reduction in power electronics and rare-earth PM materials such as currently available grades of *Nd-Fe-B* with remnant flux density exceeding 1.4 T, have narrowed the margin of the extra cost of PM motors. It is now possible to consider using these motors in applications such as pumps, fans and compressor drives, where the higher initial cost can be rapidly paid back by energy savings in a year or so [3].

It is usual, in the initial stages of a design, to calculate the air-gap flux density based on the magnet second quadrant demagnetization curve and the MMF drops in the magnetic circuit. The machine resistance and inductance values can then be used to estimate the torque and current at various speeds. However, parameter adjustments are required to allow for the saturation and armature reaction. In conventional design calculations, there is usually inadequate information on space and time variations of flux distribution. In the design of high efficiency industrial PM drives, this additional information can be provided if FE analysis is employed. The FE technique has been employed with confidence to account for saturation, space harmonics and iron losses.

The design of PM motors for high efficiency applications is centered around the trade off between mass of PM active materials and losses. A good design will minimize capital cost for a given efficiency. This formulation of the problem is used here which describes the electromagnetic design, construction and testing of a prototype 2.3 HP switched PM machine.

ASPECTS OF MOTOR DESIGN

Design is an interactive iterative process. Main factors influencing the design of a drive system are application, cost and choice of materials. Traditional methods for motor design aim at extracting maximum power from a frame size. The output is limited by the capability to dissipate heat generated by machine losses. When designing high efficiency motors, thermal issues are generally of little concern, at least in the initial design. The motors are cooled easily, because losses are much lower than in standard motors and operate with a lower

*. *Corresponding Author, Department of Electrical and Computer Engineering, Amir Kabir University, Tehran, I.R. Iran, 15914.*

1. *Department of Electrical and Computer Engineering, University of Toronto, Toronto, Canada, M5S 3G4.*

temperature rise, smaller cooling fan, or both [4]. This paper concentrates on motor design for sizes where cooling is not a major issue, probably in the range of less than 200 HP.

Torque Model

The stator of a PM motor may be identical with that of an induction motor of slightly lower rating. This paper considers three-phase switched-mode PM motors, also known as brushless DC motors, which are fed with rectangular pulses of stator current. Each phase of the stator consists of concentrated winding over two 60° sectors. If the magnets are of full width, then at any instant, each magnet interacts with 120° arc of the current carrying stator conductor. Switching of the current occurs when the magnet edge reaches the boundary between phases. Consider a phase winding with N turns per phase distributed uniformly over a 60° arc. With the current supplied to the motor, I, the linear current density for a radial airgap radius r is $\hat{K}=\frac{3NI}{\pi r}$ A/m. Since each phase is energized two-thirds of the time, the *rms* value of linear current density is $K=\sqrt{2/3}\hat{K}$ A/m. The rotor consists of the iron core, normally but not necessarily laminated, with salient magnets mounted on the periphery. Two or three radially magnetized flat magnets may be placed side by side and are fixed to the core by adhesive to create pole structure. The air-gap flux density B is maintained over the circumferential width w of the magnet or over an angular half width α. The fundamental space component B_1 of gap flux density is given by $B_1=\frac{2\sqrt{2}}{\pi}B\sin\alpha$. This component of the air-gap flux density interacts with the linear current density to produce torque in the sine-fed motor. In the rectangular-fed motor, the thrust is produced over two-thirds of the stator area. Thus, for a rotor length l the torque is:

$$T=\frac{2}{3}(2\pi rl)rB\hat{K} \quad . \tag{1}$$

It is observed that the height of the magnet h is independent of the rating of the motor. As motor torque is increased, the ratio of magnet volume to overall volume will, therefore, decrease. The ratio of the switched PM motor torque to that available from the sine-fed motor for equivalent stator currents is:

$$\frac{T_{\text{rect}}}{T_{\text{sine}}}=\frac{\pi}{2\sqrt{3}\,k_w\sin\alpha} \quad . \tag{2}$$

Substituting typical values of $\alpha = 65°$ and $k_w = 0.95$ into the above equation yields a ratio of 1.05, showing that the torque ratings of the two types of motors can be considered almost identical. This analysis ignores the effect of phase commutation on the current waveform resulting in additional torque ripple and noise. However, this factor only has a secondary effect on efficiency. Thus, for the purpose of estimating machine dimensions and efficiency, the sinusoidal model [5] can be used with little error.

Flux and Current Density Constraints

The flux and current density constraints of rectangular-fed motors can be obtained by making some minor revisions to the sinusoidal model. Following the steps in [5], one can show how r, l and the basic internal variables B and K can be chosen to provide a specified motor torque within constraints. B is limited by magnetic saturation in the stator teeth, each of width w_t, while K is limited by the slot width w_s. The product $B \times K$ in Equation 1 is maximized when about half of the stator is used for teeth and half for slots, i.e., when $w_t = w_s$. Since the maximum flux density in the teeth B_t is limited to the range 1.6-1.9 T, a reasonable value for B is in the range of 0.8-0.95 T, i.e., about 72-85% of the residual density $B_r \approx 1.1$ T for average *Nd-Fe-B*. In this paper, the constraint on the linear current density in the stator slots is the desired efficiency of the machine. However, in most designs, the applicable constraint is the maximum temperature of the stator winding insulation. There must be a balance between the ability of the cooling system to remove heat and the total losses in the stator winding and the stator core. By modifying the stator winding loss of sine-fed motors for rect-fed ones, the power loss for two phases in series of a p-pole motor with slot height h_s can now be expressed approximately as:

$$P_{sw}=\frac{2}{3}[\frac{2\pi r\rho}{f_s\gamma h_s}(l+\frac{\sigma(2\pi r)}{p})]\,K^2 \quad , \tag{3}$$

where f_s(0.3-0.5), $\gamma(\approx 0.5)$ and $\sigma(1.6-2)$ are the slot space factor, the slot width to slot pitch ratio and the ratio of the length of the overhang portion of a stator coil to the pole pitch, respectively. ρ is the conductor resistivity at the operating temperature. The copper loss constitutes the majority of the losses of the machine. For high efficiency, Equation 3 imposes a constraint on the current density.

Choice of Rotor Shape

The choice of rotor shape, defined by the l/r ratio, may be based on several criteria. One might be the shape, giving maximum torque to inertia ratio for high acceleration. For high efficiency drives, losses should be low and the stator coil should have the minimum length for the maximum gap area enclosed. This occurs for:

$$\frac{l}{r}=\frac{2\sigma\pi}{p} \quad . \tag{4}$$

The effect of the l/r ratio on iron volume is different. The ratio of iron volume in the teeth to

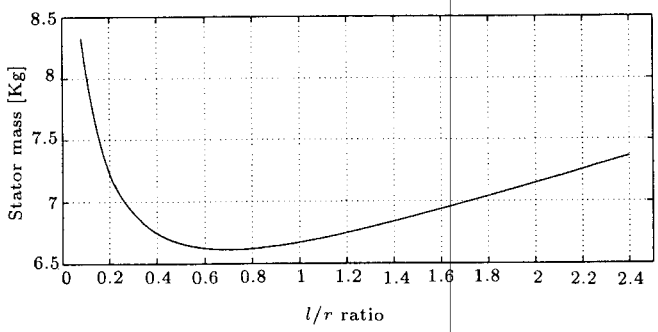

Figure 1. Sensitivity of stator mass to l/r ratio for an 8-pole motor under constant per unit copper loss.

torque decreases continuously with the l/r ratio. This happens because the tooth volume is proportional only to the active air-gap surface area and none of it is wasted as in the case with copper. Thus, from the point of view of minimizing stator core, the l/r should be made as low as possible. For this reason, the optimum l/r ratio is lower than indicated in Equation 4. Figure 1 illustrates the variation of stator mass with l/r ratio for an 8 pole motor under the condition of constant per unit copper loss. The graph demonstrates that the sensitivity is small for a wide variation beyond the minimum value.

Core Loss Model and Saturation

The yoke thickness and core loss model for PM machines have been described in [5]. It can be shown that the ratio of yoke height h_y to rotor diameter D is:

$$\frac{h_y}{D} = \frac{\alpha B}{pB_y} \quad . \tag{5}$$

Typically, the maximum yoke flux density B_y is chosen in the range 1.4-1.7 T but can be varied to adjust the core loss. The accurate calculation of core loss in PM machines still presents some difficulties. In a surface-mounted PM motor with a magnet of constant height, the stator flux density variations are far from sinusoidal. The tooth flux density rises rapidly as the magnet edge crosses the tooth face and then remains constant as the magnet passes. This rapid rate of change does not affect the hysteresis loss but is critical for eddy currents. It was illustrated that in an S slot machine operating with radian frequency ω_s and maximum tooth flux density B_t, the total core loss in the stator teeth P_{ct} and the yoke core loss P_{cy} may be approximated by:

$$P_{ct} = \pi l h_s (1-\gamma)(2r + bh_s) \times \left[k_h B_t^n \omega_s + \frac{4k_e S}{\pi^2 p(1-\gamma)}(B_t\omega_s)^2\right] , \tag{6}$$

$$P_{cy} = 2\pi l h_y (r + h_s + h_y/2)\left[k_h B_y^n \omega_s + \frac{4k_e}{\pi\alpha}(B_y\omega_s)^2\right], \tag{7}$$

where $b = 1$ for parallel-sided slots and $b = 0$ for parallel-sided teeth. The loss constants k_h, k_e and n are determined by curve fitting to the measured core loss data obtained for the proper grade of silicon iron laminations. The tooth and yoke flux densities vary by the addition of leakage flux due to stator current. Additional eddy current losses will also occur at the interface region of yoke and teeth. These losses, as well as those in the lip, are difficult to estimate by analytical methods. Finite element analysis should be used to accurately determine the eddy current losses. To avoid saturation and high core losses in a PM motor, detailed distribution of flux density in the stator is needed. With FE method, the flux distribution in the stator can be clearly seen in Figure 2 and core losses in the teeth and the yoke calculated by the following equations.

$$P_{ct} = \varrho_i k_h l \omega_s \sum_{e=1}^{E_t} \triangle_e B_{t,e}^n + \frac{\omega_s^2}{2\pi^2}\varrho_i k_e l \times \sum_{e=1}^{E_t} \triangle_e \left[\sum_{m=1}^{M} (B_{t,e,m} - B_{t,e,m-1})^2\right], \tag{8}$$

$$P_{cy} = \varrho_i k_h l \omega_s \sum_{e=1}^{E_y} \triangle_e B_{y,e}^n + \frac{\omega_s^2}{2\pi^2}\varrho_i k_e l \times \sum_{e=1}^{E_y} \triangle_e \left[\sum_{m=1}^{M} (B_{y,e,m} - B_{y,e,m-1})^2\right], \tag{9}$$

where ϱ_i and $\triangle_e$ are the mass density of iron and the area of each element, respectively. The subscripts e and

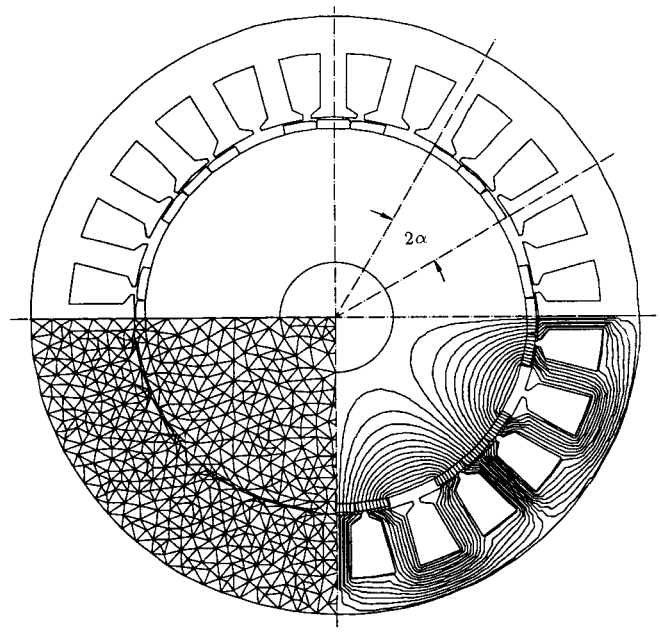

Figure 2. Cross section, mesh and flux lines in the experimental PM motor.

m stand for the element number and the step number used in solving the field problem by FE method.

In an induction motor, stray losses due to interaction of stator and rotor teeth are significant. It has been experimentally established that this class of loss is negligible in surface-mounted PM motors [6]. To complete the loss determination, there is, of course, a component of friction and windage P_{fw}.

DESIGN GUIDELINES AND CONSTRUCTION

PM motor designs were examined using the algebraic formulation of PMDESIGN, a PM motor sizing and simulation computer program written by the authors. FE analysis studies subsequently verified PMDESIGN results.

Magnets

Neodymium (Neo), Samarium and Ferrite magnets are the available materials best suited for use in general purpose PM motors. Neo magnet has higher residual flux density and coercivity compared with the other two. It is also cheaper than Samarium magnet, but the maximum temperature of operation is $\sim$ 150°C which is lower than $\sim$ 380°C or Samarium magnet. This is, however, not a serious matter in most PM machine designs since the magnets are not located in a region of significant power loss and the cooling air exit temperature is usually below 100°C. These materials are to be compared on the basis of torque output per unit of rotor volume, T_v, which according to Equation 1 is proportional to $B \times K$. B is $\sim$ 75% of the magnet residual density B_r. As discussed before, B is limited not only by B_r, but also by B_t. For low loss silicon steel, B_t ~1.6 T. This necessitates that the ratio of tooth width to slot pitch, $w_t/(w_t + w_s)$, must be $B/(1.6\ \mathrm{T})$. K can be assumed to be proportional to w_s, since the current carrying copper is located in the slot. Hence, T_v is proportional to $w_t w_s$. The results for different magnets are summarized in Table 1, where (w_t+w_s) is taken as 1 per unit. It is observed that if the operating temperature of machine is less than 150°C, which usually is the case, Neo machine costs much less than Samarium one for the same T_v. The Ferrite magnet is very cheap, but would require significantly larger machine size for equivalent power output. The table also shows that even though the bonded Neo magnet has only 64% of the B_r of the sintered Neo, it can produce 87% of T_v. Moreover, its relative cost is almost 75% of the sintered Neo. Thus, bonded Neo magnet is a good choice for PM motors. It can be concluded that the margin of increased performance of the bonded Neo over the Ferrite magnet is much larger than that of the sintered Neo over the bonded Neo.

Number of Slots

The number of slots has an important effect on the teeth eddy current loss. For a given supply frequency, this loss is proportional to the number of slots. This results from the rapid change of flux as the magnet passes over a narrow teeth. Hence, it is beneficial to use fewer but wider teeth. An alternative solution to the problem of high eddy losses in the teeth is to magnetize the magnets in a gradual flux increase from the edges to the middle. This solves the problem, but results in some of the expensive magnet being not fully utilized. The required number of slots depends also on the winding distribution. In concentrated winding switched-mode excitation, it is possible to use only one slot per pole-phase.

Number of Poles

Variable speed inverter-driven motors are free from the number of poles constraint imposed on AC motors operating directly off the fixed line frequency. The inverter can output any frequency required, up to several hundred Hz for the modern fast switching IGBT powered units. This allows p to be selected for best

Table 1. Significant properties of some permanent magnets.

Material (Grade)	Max. Op. Temp. [C]	Rel. Cost per Kg	B_r [T]	H_c $[\frac{MA}{m}]$	B_g [T]	T_v [%]
Ferrite	250	5	0.40	0.18	0.30	60.9
Bonded Neo(B10N)	150	60	0.68	0.45	0.51	86.8
Sintered Neo(27H)	150	80	1.06	0.79	0.79	100
Sintered Neo(39H)	150	80	1.28	0.97	0.96	96.0
Sintered Neo(45H)	100	90	1.35	1.01	1.0	92.8
Sintered Neo(48)	80	90	1.41	1.01	1.1	89.6
Sm-Co(26HS)	380	130	1.06	0.77	0.79	100
Sm-Co(32H)	350	140	1.16	0.75	0.87	99.2

motor design. The following direct benefits occur by increasing p in a motor:

- The length of the end turn windings and, thus, the stator winding copper loss, Equation 3, is inversely proportional to p.
- The stator yoke height, Equation 5, is inversely proportional to p as well.
- To a first approximation, the optimum ratio of air-gap radius/length increases proportional to p, Equation 4.

These features reduce the mass of copper and iron required. Overall, as shown in Figure 3, the total mass of active materials is typically reduced by almost half when p is changed from 4 to 8. One potential problem of increasing p is its effect on the motor's iron loss. The total effect is determined by the ratio of hysteresis to eddy current loss. If hysteresis loss dominates, increasing p will not raise the total iron loss much. This is the case even though the loss per unit volume increases as p, because the iron volume drops almost as the inverse of p. However, when eddy current loss dominates, the total iron loss is likely to increase as p even after considering the reduced volume. Thus, from the perspective of iron loss, it is beneficial to increase p if iron with low eddy current to hysteresis loss ratio at the frequency used is available. Figure 3 shows an example of the effect of changing p on total losses in 0.35 mm laminations of M15 steel, under the condition of constant copper loss.

Another important consideration when increasing the number of poles is the effect on the optimum air-gap length/radius ratio. With 4 poles, the optimum is $\sim$ 2.5, while with 8 poles it drops to $\sim$ 1.25. As the pole count grows even higher, the optimum motor shape begins to resemble a pancake. This is a problem

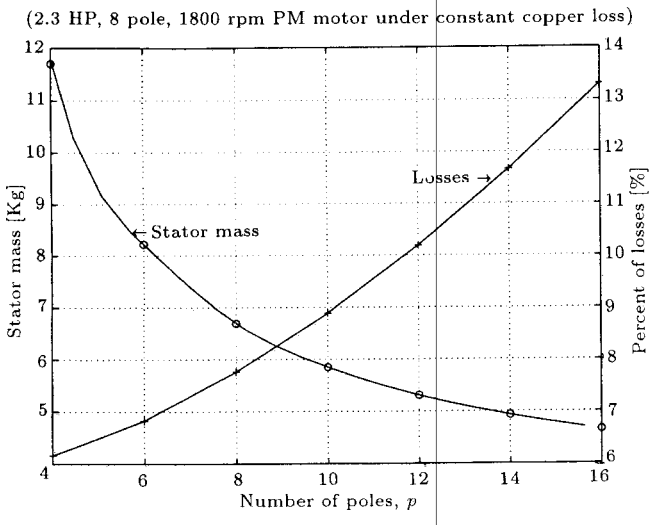

Figure 3. Sensitivity of stator mass and losses to number of poles.

because the standard motor frames are not designed in this way. Hence, in order to use regular motor frames, a practical limit of 8 or 10 is imposed on p.

Experimental Machine Construction

To verify the expected benefits of PM motors incorporating the features outlined in this paper, a 2.3 HP prototype was designed and constructed inside a standard 145 T induction motor frame. An outer stator diameter constraint of 160 mm and an estimated constraint of 60 mm on the stack length were, therefore, imposed. A cross section of the stator and the rotor is shown in Figure 2. The significant dimensions and properties of the prototype are listed in the Appendix. The key distinguishing characteristics of the motor were as follows:

a) The machine was designed with 8 poles and 1 slot per pole-phase with concentrated windings.

b) M19 grade steel with 0.65 mm laminations and low loss M15 grade steel with 0.35 mm laminations were used on the rotor and the stator, respectively.

c) Grade 27H sintered Neo were used, even though it was concluded that bonded ones were the economical choice. This choice was made only because the sintered magnets in the particular size and shape were more easily available.

Testing

One aspect of lab testing was to verify the core loss prediction. Core loss occurs when the stator is open circuited because of the PM excitation and the rotation of the rotor. To obtain a measure of the core loss, the open-circuited machine was driven by a small dynamometer and the shaft torque was measured over a range of speed. The torque-speed product then represented the no load loss of the motor consisting of the sum of the core loss, as well as the friction and windage losses P_{fw}. This latter component of loss cannot be measured directly on a PM motor since the field-produced core loss is always present. Formula predicting P_{fw} of rotating masses are theoretical functions approximated with practical results. Meriam [7] uses the formula $P_b = 2\pi\nu r_b^3 l_b \omega^2 / g_b$ for the journal bearing friction loss, where ν is the coefficient of viscosity of fluid and subscript b stands for bearing. James and Alzahawi [8] quote a formula for the loss due to friction drag on the cylindrical surface of a machine, P_{cyl}, based on theoretical extrapolation of experimental data. The formula is:

$$P_{cyl} = 0.5\pi\varrho r^4 \omega^3 l c \quad , \tag{10}$$

where ϱ, ω and c are density of the surrounding air, rotational speed of the rotor and drag coefficient, respectively. c is a function of Reynolds number [9]. For a fluid surrounding the radial surface of a cylindrical

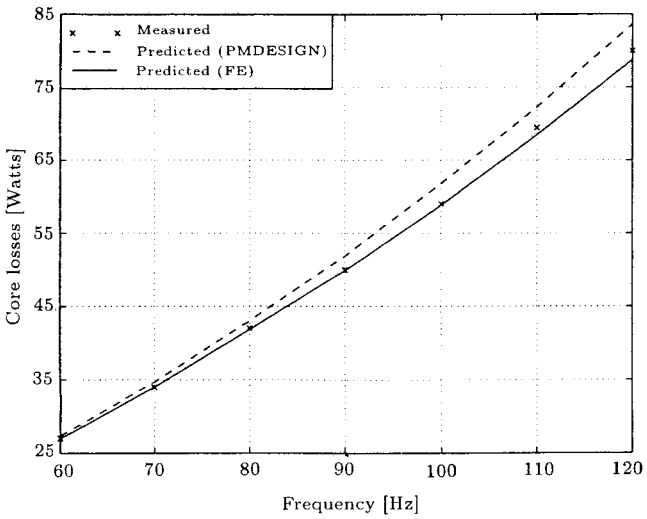

Figure 4. Comparison of core losses in the 2.3 HP prototype motor.

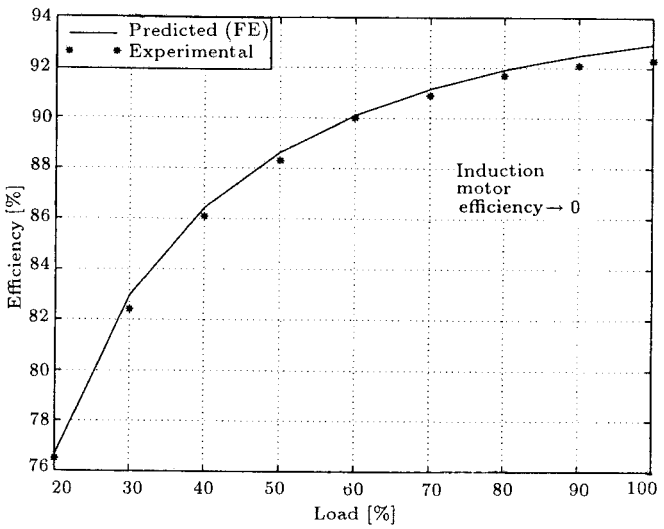

Figure 5. Comparison of the predicted and the experimental efficiencies of the 2.3 HP prototype motor at 1800 rpm.

surface of a cylindrical machine, Reynolds number is $\varrho\omega rg/\nu$, where g is the radial air-gap length. Friction and windage losses, $P_{fw} = P_{cyl} + P_b$, subtracted from the total mechanical input power gave the core loss as a function of speed. The experimental core loss data is compared with the predicted ones using PMDESIGN (Equations 6 and 7) and FE analysis (Equations 8 and 9) in Figure 4. The correspondence was close for frequencies less than 120 Hz, the difference being within the estimated experimental error band. At higher frequencies, the FE method is suggested. Besides the core loss test, the machine was tested at load to confirm the expected torque per amp of stator current. Copper loss was calculated from the measured resistance of the winding at operating temperature. The tests gave enough data to compute efficiency. The results together with the predicted values are plotted in Figure 5. The experimentally determined efficiency of the PM motor at 2 HP was 92.1%, which was much higher than the 86.2% efficiency for the typical energy efficient induction motor whose frame was used for the prototype. The theoretical efficiency was 92.5%.

CONCLUSION

This paper has described the design, construction and testing of a switched-mode PM motor which has incorporated the guidelines meant to reduce cost and active material consumption producing a high efficiency industrial machine. The choice of magnetic material, number of slots and number of poles have been identified as critical to achieving this goal. Through sensitivity studies of these elements, more economical design of PM motors has been made possible for use with inverters in variable-speed drives. In industrial drive applications, owing to their high flux density and coercivity, $Nd - Fe - B$ will be preferred for mass products. Due to its high cost, Sm-Co can be useful only in machines with high temperatures. The 2.3 HP, 3-phase prototype has achieved significantly higher efficiency than all known switched-reluctance and induction motor drives constructed in the same frame size. It may be concluded that the cost of the relatively expensive Neo magnet material is recovered many times over by the reduced losses.

There are still some uncertainties regarding the contribution of high frequency fields to eddy current losses. The authors are now studying different methods to model the iron losses and the effects of saturation more accurately, which will be presented in a later occasion.

REFERENCES

1. Buschow, K.H.J. "New permanent-magnet materials", *Material Science Report*, **1** (Sept. 1986).

2. Sebastianm, T. and Slemon, G.R. "Transient torque and short circuit capabilities of variable speed permanent magnet motors", *IEEE Trans. Magn.*, **Mag-23**, pp 3619-3621 (Sept. 1987).

3. Nadel, S. et al. *Energy Efficient Motor Systems' Handbook*, American Council for an Energy Efficient Economy (1991).

4. Wilson, J.H. and Herzel, J.C. "Design and comparison of energy efficient motors", *IEEE Canadian Review*, pp 17-18 (Winter 1992).

5. Slemon, G.R. and Liu, X. "Modeling and design optimization of permanent magnet motors", *Electric Machines and Power Systems*, **20**, pp 71-92 (1992).

6. Sebastian, T. and Slemon, G.R. "Transient modeling and performance of variable speed PM motors", *IEEE Trans. Ind. App.*, **IA-25**, pp 101-107 (Jan/Feb 1989).
7. Meriam, J.L., *Statics*, New York, John Wiley (1975).
8. James, B.P. and Alzahawi, B.A.T. "A high speed alternator for small scale gas turbine CHP unit", *IEE 7th Inter. Conf. Electrical Machines and Drives*, pp 281-285 (Sept. 1995).
9. Sumer, B.M. and Fredsoe, J., *Hydrodynamics Around Cylindrical Structure*, New York, World Scientific (1997).

APPENDIX

The machine was a 3-phase, 230-v, rectangular-fed, 8-pole, 24-slot, surface-mounted magnet, radial-field PM motor. The design parameters are listed in Table A1.

Table A1. Specifications of the prototype motor.

Parameter	Value
Angular width of magnet (2α)	130°
Outer radius of stator	80.0 mm
Airgap radius	53.0 mm
Airgap length	0.65 mm
Stack length	57.0 mm
Tooth width	6.90 mm
Magnet height	2.30 mm
Slot fill factor	40.5%
Magnet weight	0.23 Kg
Copper weight	1.80 Kg
Stator teeth iron	1.24 Kg
Stator yoke iron	2.06 Kg